Arch. Metall. Mater. **68** (2023), 2, 431-438

DOI: https://doi.org/10.24425/amm.2023.142419

A.G. LUK'YANENKO[1*], I.M. POHRELYUK[1], V.M. FEDIRKO[1],
A.G. MOLYAR[2], V.S. TRUSH[1], T.M. KRAVCHYSHYN[1]

GAS NITRIDING OF THE NEAR-BETA-TITANIUM ALLOY

The present research investigates the nitriding kinetics of the near-beta-titanium alloy of Ti-Al-Nb-Fe-Zr-Mo-V system at 750, 800, and 850°C in gaseous nitrogen at 10^5 Pa for 2, 4, and 8 h. The parabolic coefficient k_p of the layer's growth rate and the nitriding activation energy E are set as the kinetic parameters of the nitrided layer's growth. The activation energy for the formation of a nitride layer is ~108 kJ/mol. The authors discuss the morphology of the nitride layers as well as their roughness and surface hardness. The study determines the effective diffusion coefficient for the growth of diffusion layers in the temperature range of 750...850°C: $D_{ef} = D_0 \times \exp(-E/RT)$, where $D_0 = 0.0177$ m^2/s; $E = 215.7$ kJ/mol. The friction coefficient of the disk from near-beta-titanium alloy with a bronze block is lowered by significantly more than 10 times after gas nitriding, and the temperature in the friction zone is reduced by 2.5 times.

Keywords: near-beta-titanium alloy; nitriding; kinetics; diffusion; microhardness

1. Introduction

The most widely used materials in aeronautical, engineering, and biomedical application are biphasic high strength near-beta-titanium alloys due to their high specific strength [1-4]. Fuselage parts, wings, chassis, control system parts, aircraft power elements, including welded parts, fasteners, and the like are fabricated from such alloys [1,3]. However, the reliability of titanium alloy parts in manufacturing is generally limited not only by the material's strength but also by its low tribological properties [5].

A number of works describe different methods of nitriding [6], Ion Nitriding [7], Plasma Nitriding [8], Laser-Assisted Nitriding [9], Gas-Blow Induction Heating Nitriding Method [10], Electron-Beam Vacuum Nitriding [11], Physical Vapor Deposition (PVD) [12] and Chemical Vapor Deposition (CVD) methods [13] and Gas Nitriding [6]. The main difference of these methods from traditional gas nitriding in most cases is that the nitride layer is formed from the surface outward, while in gas nitriding the nitride layer is mainly formed with the involvement of the inner layers of the metal being processed. Traditional diffusion nitriding remains a promising, efficient, and economically reasonable method of thermochemical treatment among the other surface hardening methods that increase the wear and fretting resistance of titanium alloys [14-16]. This method is technologically simple, provides stable physicochemical characteristics of treated surfaces, has no other technological operations, is easily reproduced, and allows the processing of complicated shape details. The formation of transitory diffusion layers during gas nitriding ensures the strong adhesion of the surface nitride layer to the matrix. Nitriding may be used in the thermal treatment of parts made of near-beta-titanium alloys as needed [17]. In our study, we tried to obtain the maximum effect from surface treatment (nitriding) with a minimum effect on the structure of the metal volume. That is, to obtain hardened near-surface metal layers with acceptable characteristics at temperatures below the temperature of $\alpha \leftrightarrow \beta$ polymorphic transformation, i.e. in our case below a temperature of 850°C. Thus, our results show that nitriding at temperatures of 750-800°C for up to 8 hours forms an acceptable hardened layer with minimal effect on the matrix microstructure. Also, such nitriding modes can be integrated with hardening heat treatment of products from such an alloy, as was shown in the works [6,18]. As a result, the objective of this study is to look into the regularities of surface hardening

[1] G.V. KARPENKO PHYSICO-MECHANICS INSTITUTE OF THE NAS OF UKRAINE, DEPARTMENT OF MATERIAL SCIENCE BASES OF SURFACE ENGINEERING, 5, NAUKOVA STR., 79060 LVIV, UKRAINE
[2] G.V. KURDYUMOV INSTITUTE FOR METAL PHYSICS OF THE NAS OF UKRAINE, DEPARTMENT OF PHYSICS OF STRENGTH AND DUCTILITY OF INHOMOGENEOUS ALLOYS, 36 ACADEMICIAN VERNADSKY BOULEVARD, 03142 KYIV, UKRAINE

* Corresponding author: alukanenko246@gmail.com

of high-strength near-beta-titanium alloys from the Ti-Al-V-Mo-Zr-Fe-Nb system after thermochemical treatment in nitrogen at 10^5 Pa for 2, 4, and 8 h at 750, 800, and 850°C.

2. Material and methods

TABLE 1 presents the chemical composition and mechanical properties of experimental high-strength (β-rich α + β- or near-beta- because the coefficient of stabilization of the beta phase is MoE = 1.72...5.21, according to [1]) titanium alloy (named FT01 below) of the Ti-Al-Nb-Fe-Zr-Mo-V alloying system (manufactured by the People's Republic of China). To study the kinetics and structural state of the metal, X-ray and durometric studies, flat samples of 15×10×1 mm were used. At least 7 samples per point were used in the nitriding kinetics study. To determine the friction coefficient, the disk samples with outer diameter of 38 mm and a thickness of 10 mm were used.

For nitriding, the researchers used vacuum heat treatment equipment with controlled gas environments. The saturation temperature was 750°C, 800°C, and 850°C, respectively. Saturation durations were 2, 4, and 8 h. The pressure of nitrogen was 10^5 Pa. During the heating stage, specimens were heated to a nitriding temperature in a 1×10^{-3} Pa pressure to remove natural oxide films and prevent new ones from forming. The heating rate was 2.5°C/min. After isothermal soaking in nitrogen, samples were cooled to 500°C in nitrogen in the furnace (at an average cooling rate of 1.68°C/min) before the system was degassed. The used nitrogen gas was of technical grade purity, including no more than 0.4 vol.% oxygen and no more than 0.07 g/m^3 water vapor. Nitrogen was routed through the silica gel capsule and titanium chips, which heated to 50°C above nitriding temperature, before being injected into the furnace's reaction space.

The samples were weighed to a precision of ±0.0001 g on analytical balances OHAUS Voyager V 10640. The researchers determined the phase composition of the alloy's surface layers after nitriding through X-ray phase analysis using a DRON-3.0 X-ray diffractometer in monochromatic $Cu_{K\alpha}$-radiation with Bragg-Brentano focusing. The anode of the x-ray tube had a voltage of 30 kV and a current of 20 mA. Special software programs helped identify the position of the diffraction peaks and compare them to JCPDS-ASTM data for the Fourier diffraction.

The surface roughness of alloy specimens was measured before and after nitriding using a profilometer model 176021 with automatic determination of the arithmetic mean deviation of the profile *Ra* (μm) by GOST 2789-73. The researchers prepared metallographic specimens of nitrided titanium alloy according to the standard method for microstructural and durometric measurements; the structure was detected by etching Kroll's reagent (3 ml HF, 6 ml HNO_3 in 100 ml distilled water). The authors were using an EPIQUANT microscope with an eTREK DCM520 digital ocular camera and standard software and an EVO 40XVP scanning electron microscope with an INCA Energy microanalysis system to perform microstructural analyses.

The degree of near-surface nitrogen saturation of the alloy was determined by measuring the distribution of microhardness on the metallographic cross-section of the sample using PMT-3M microhardness gauge under load on the indenter 0.49 and 0.98 N. The distributions of microhardness over the cross-section of samples were examined by "beveled sample" sections, which had been cut at a ~15° angle, enabling the hardened zone to expand three times and therefore improving parameter determination accuracy. The depth of the hardened layer was taken the thickness of the metal, which had a higher hardness than the hardness of the alloy matrix on $\Delta H = 0.2$ GPa.

The authors conducted tribotechnical analyses on a 10,000 m base using an SMC-2 friction machine and the "block-on-ring" scheme with a specific load of 0.6 MPa and a sliding speed of 0.625 m/s. Disks of FT01 alloy were tested, the surface of which had no strengthening and was hardened by nitriding. BrAZhN 10-4-4 deformed bronze was used to make the block. The friction pair was lubricated by immersing it in a cuvette with AMG-10 aviation hydraulic fluid (TU U 23.2-20574128-066:2007). The wear resistance of hardened alloy was measured by weighing it on Voyager (OHAUS) balances to evaluate the changes in friction coefficient and mass during friction by GOST 23.224–86.

3. Results and discussion

The alloy samples have two-phased lamellae and textured structures in their initial state (Fig. 1a, b). During the fabrication of the semi-finished product, a minimal hardness gradient is formed in the thin surface layers H^s = 382±19 $HV_{0.49}$ (3.74±0.18 GPa) and H^s = 374±15 $HV_{0.98}$ (3.66±15 GPa). The matrix had a hardness of H^m = 433±29 $HV_{0.49}$ (4.24±0.28 GPa). In the production of pipe blanks, to prevent oxidation and reduce friction during rolling, as a rule, protective lubricants are used,

TABLE 1

The chemical composition and mechanical properties of FT01 titanium alloy

The chemical composition, mas. %									
Alloying elements						Impurities, not more			Base
Al	Nb	Fe	Zr	Mo	V	O_2	H_2	N_2	Ti
5.0… 6.5	2.5… 4.0	1.5… 2.5	0.5… 2.5	1.0… 2.0	1.0… 2.0	0.1	0.01	0.05	balance
The mechanical properties									
Thermal treatment	Ultimate Tensile Strength σ_{UTS}, MPa		Yield stress σ_y, MPa			δ, %	ψ, %		KCU, J/cm^2
Annealing	1100…1250		1000…1200			15	35		30

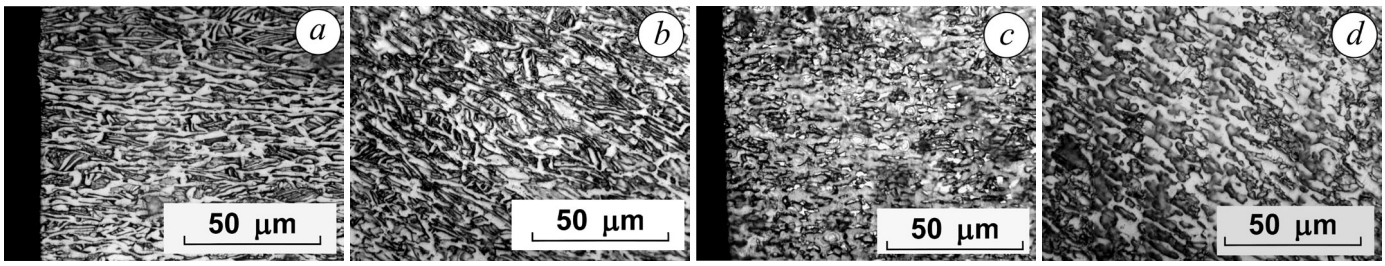

Fig. 1. The structure of the FT01 alloy's near-surface layers (*a*, *c*) and matrix (*b*, *d*) in the initial state (*a*, *b*) and after vacuum annealing (*c*, *d*)

which are removed by chemical pickling, and intermediate annealing, as a rule, are vacuum annealing to remove hardening of metal. As a result of such operations, the surface layer of the metal of the pipe billet may lose an insignificant part of the alloying elements, which leads to a somewhat lower hardness compared to the hardness of the matrix. Homogenizing annealing eliminates this effect in general.

The samples were annealed at 800°C in a vacuum for 2 h to create the initial phase-structural state (removal of hydrogen, structure homogenization and stabilization, and complete removal of residual stresses). Fig. 1c, d shows the structure of the samples after annealing. The surface microhardness was H^s = 362±10 $HV_{0.49}$ (3.55±0.10 GPa) and H^s = 361±15 $HV_{0.98}$ (3.54±0.15 GPa) after annealing, at the matrix hardness was H^m = 376±13 $HV_{0.49}$ (3.68±0.13 GPa). Hardened layers are formed as a result of nitrogen dissolving in the matrix and chemically reacting with titanium alloy, and it includes a surface phase film (TiN_x and Ti_2N nitrides) (Fig. 2, zone *1*) and a diffusion zone (nitrogen dissolution in titanium, Fig. 2, zone *5*), which is observed between the nitride layer and the alloy matrix, as confirmed by X-ray, metallographic, and microhardness tests.

After nitriding in the tested temperature range (750...850°C) and exposure time frame (2...8 h), the surface of the alloy acquires a light golden color due to the nitride film. According to X-ray phase analysis, the film consists of the basic titanium nitrides – δ-nitride TiN_x and ε-nitride Ti_2N (Fig. 3). No data on the formation of nitrides of other compositions or alloying elements currently exists. Titanium nitride TiN_x is characterized by a low number and intensity of reflections in diffraction spectra taken from the sample's nitrided surface. Temperature and nitriding duration increases the density and intensity of reflections. After 8 h of exposure, the cubic lattice parameter of TiN_x on the surface of the samples increases from 0.4255 to 0.4260 nm as the temperature rises from 750 to 850°C. As saturation time at 850°C extends from 2 to 8 h, the TiN_x cubic lattice parameter increases from 0.4257 to 0.4260 nm.

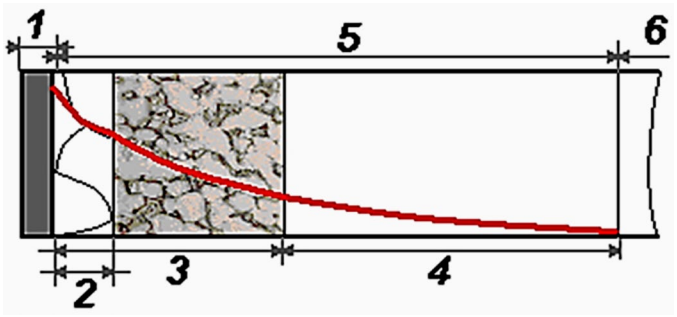

Fig. 2. The structure of surface and near-surface hardened layers on FT01 alloy after nitriding (diagram): *1* – the layer of nitride ($\lambda_{TiN+Ti2N}$); *2* – the layer of the solid solution of nitrogen in α-titanium (λ_α); *3* – the layer of the solid solution of nitrogen in $\alpha + \beta$ titanium with structural changes (λ_S); *4* – the layer of the solid solution of nitrogen in the metal without any obvious structural changes; *5* – the metal layers hardened by nitrogen in general (λ_H); *6* – alloy matrix (the red curve indicates the distribution of microhardness across the section)

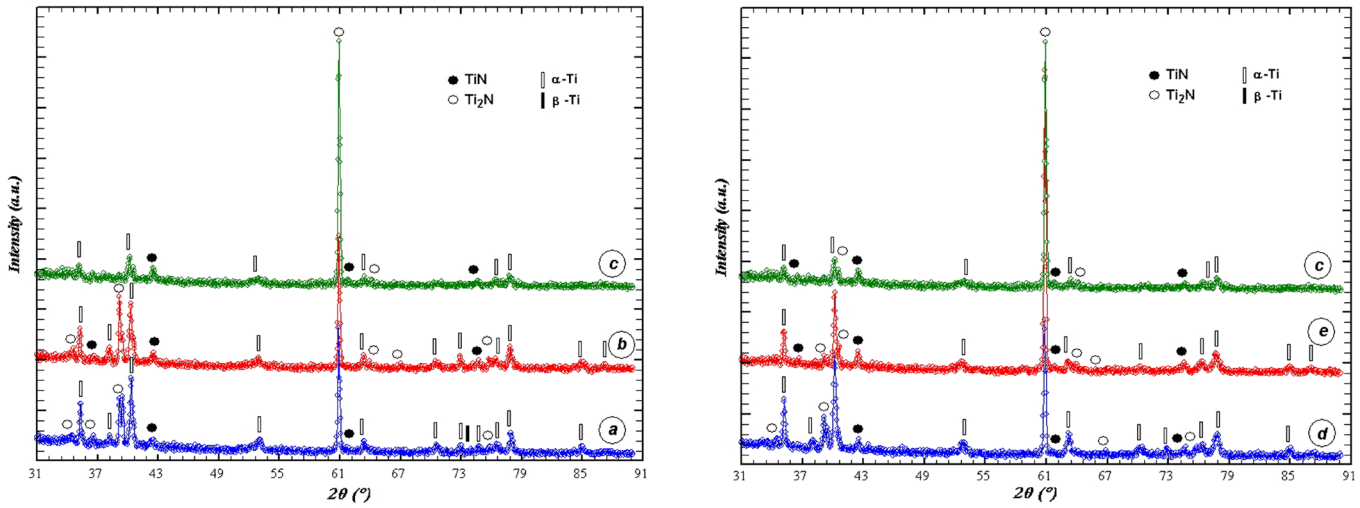

Fig. 3. The resulting diffraction data recorded from the surface of the FT01 titanium alloy after nitriding at nitrogen pressure $P_{N2} = 10^5$ Pa for the following temperatures and periods: *a* – 750°C, 8 h; *b* – 800°C, 8 h; *c* – 850°C, 8 h; *d* – 850°C, 2 h; *e* – 850°C, 4 h

The diffraction spectrum of lower titanium nitride Ti_2N was dominated by lines (111) ($2\theta = 39°12'$) and (002) ($2\theta = 60°36'$) (See Fig. 3). The researches note that nitride prefers to be orientated in the [002] direction; this inclination increases with nitriding temperature and duration. An increase in the intensity of nitride phase reflexes occurred against the background of a decrease in the intensity of α-titanium phase reflexes. This phenomenon shows that raising the temperature-time parameters of nitriding causes the nitride film to thicken.

The thickness of the nitride film after nitriding in the studied temperature-time parameters is 1...5 μm, according to the results of the metallographic analysis. The growth of the nitride layer $\lambda_{TiN+Ti2N}$ (Fig. 4) follows the parabolic law $(\lambda_{TiN+Ti2N})^2 \approx k_p \times \tau$, where k_p is the constant of the nitride layer's parabolic growth rate, μm^2/h, and τ is the time, h. Arrhenius' law [7,10] defines the temperature dependence of the parabolic growth rate of the nitride layer as $k_p = k_0 \times \exp(-E/RT)$, where k_0 is the before-the-exponential coefficient, μm^2/h; E is the process activation energy, J/mol; R is a gas constant, R = 8,314 J/(K×mol); T is the temperature, K. This calculation allows one to estimate the activation energy of nitride layer growth at nitrogen pressure of 10^5 Pa and temperatures ranging from 750 to 850°C (Fig. 5). The calculated activation energy of nitride layer growth is E = 108 kJ/mol, and the before-the-exponential coefficient is $k_0 = 8 \times 10^6$ μm^2/h.

The formation of a specific surface topography (a relief grid that repeats the grain boundaries of titanium matrix) on the surface of FT01 alloy specimens during gas nitriding degrades its quality (Fig. 6). Parameter *Ra*, the arithmetic mean deviation of the surface profile, rises as the nitriding temperature and isothermal soaking duration grow (TABLE 2). Moreover, in the studied temperature-time range of nitriding, the maximum *Ra* values were recorded at the maximum temperature-time parameters of processing. The initial surface roughness *Ra* = 0.08...0.16 μm of samples, which corresponds to the 10th class of surface roughness, worsened after nitriding at 850°C in the studied time range (surface quality deteriorates by two classes). Surface roughness within one class tends to worsen after no more than 4 h of nitriding at 750°C. Greater exposure decreases the surface quality of another class. After nitriding at 800°C, a similar dynamic is observed: the surface roughness is increased by one class (9...8 vs. 10...9, TABLE 2). Thus, increasing the temperature from 750 to 850°C over an 8-hour nitriding exposure increases surface roughness significantly more (by two classes) than increasing the isothermal soaking duration from 2 to 8 h at the same temperatures (on the one class).

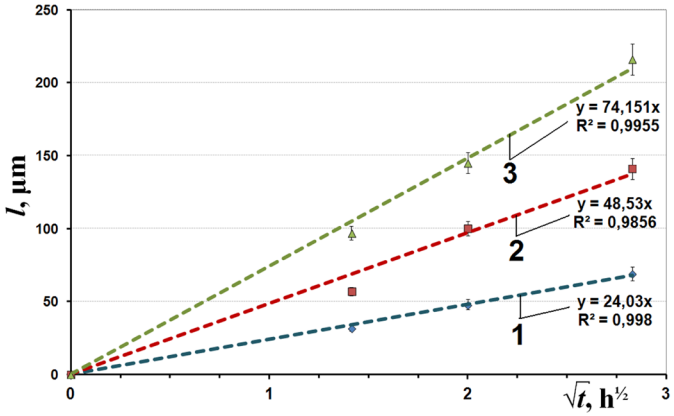

Fig. 4. Growth kinetics of a $\lambda_{TiN+Ti2N}$ nitride layer on FT01 titanium alloy in interaction with gaseous nitrogen at 10^5 Pa and temperatures: 1 – 750°C; 2 – 800°C; 3 – 850°C

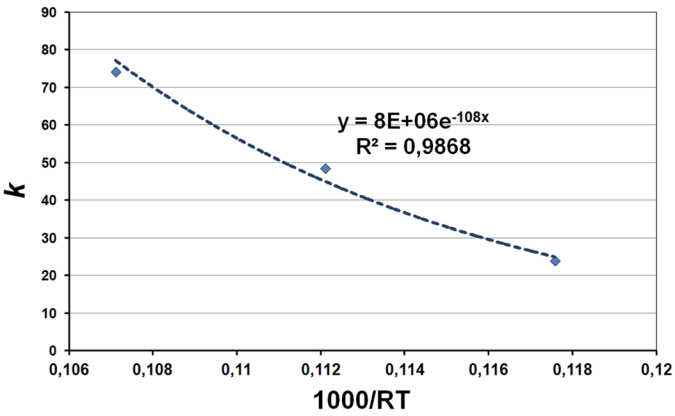

Fig. 5. Determination of activation energy of nitride layer growth on FT01 titanium alloy

The microhardness of the metal surface after nitriding (TABLE 3) rises as the nitriding temperature-time parameters grow and is higher at 0.49 N than at 0.98 N, demonstrating a gradient of surface hardening specific to diffusion processes. Under the studied temperature-time parameters, the alloy surface microhardness is within 7...16 GPa after nitriding.

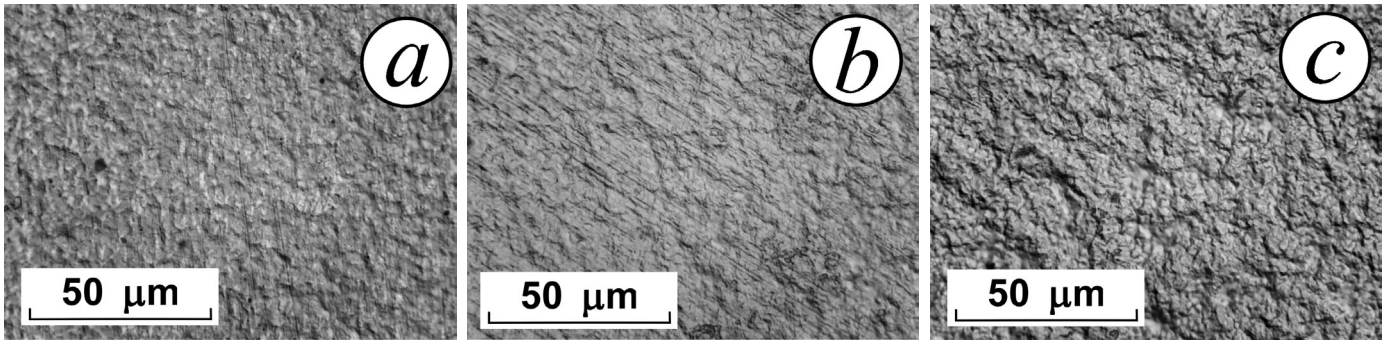

Fig. 6. Surface micrograph of FT01 titanium alloy after nitriding at nitrogen pressure $P_{N2} = 10^5$ Pa and process temperatures and durations: *a* – 750°C, 4 h; *b* – 800°C, 4 h; *c* – 850°C, 4 h

TABLE 2

The arithmetic mean deviation of the FT01 titanium alloy's surface profile *Ra* (μm) and roughness class after nitriding

Duration, h	Parameters	Temperature,°C		
		750	800	850
2	*Ra*, μm	0.143	0.244	0.548
	roughness	10 class	9 class	8 class
4	*Ra*, μm	0.159	0.259	0.535
	roughness	10 class	9 class	8 class
8	*Ra*, μm	0.168	0.356	0.576
	roughness	9 class	8 class	8 class

TABLE 3

The microhardness of the surface (H^s, GPa) of FT01 titanium alloy depending on the temperature and duration of nitriding

Duration of nitriding, h	Measurements for load, N	The microhardness of the surface (H^s, GPa) after nitriding at temperature,°C		
		750	800	850
2	0.49	8.20 ± 0.42	8.56 ± 0.41	12.28 ± 0.90
	0.98	7.58 ± 0.72	7.95 ± 0.37	9.91 ± 0.47
4	0.49	8.64 ± 0.55	9.22 ± 0.54	12.57 ± 0.94
	0.98	7.60 ± 0.30	8.69 ± 0.36	10.18 ± 0.84
8	0.49	9.23 ± 0.28	11.17 ± 0.84	15.65 ± 0.51
	0.98	7.70 ± 0.60	10.13 ± 0.57	13.04 ± 0.54

As the temperature and saturation parameters grow, the diffusion layer (the layer of solid nitrogen solution in titanium, λ_H in Fig. 2, zone *5*) enlarges, as determined by the microhardness test. Its structurally sensitive components λ_α and λ_S, the sizes of which were metallographically analyzed, thicken in a similar fashion (Fig. 7). The near-surface structural elements (Fig. 7) and alloy matrix elements (Fig. 8) also enlarge after saturation at temperatures of 750 and 800°C. By analogy with other metastable titanium alloys, the temperature of the polymorphic $\alpha \leftrightarrow \beta$ transformation for the alloy under study is ~800…850°C [19], as evidenced by the characteristic change in the microstructure of the alloy matrix after heat treatment at 850°C. The alloy matrix has a basket weaving structure after saturation at 850°C.

The growth kinetics of gas-saturated layers, as a result of nitrogen diffusion dissolution in titanium, follow the classic diffusion law [20]: $l^2 \approx D \times \tau$ (Fig. 9), where l is the dif-

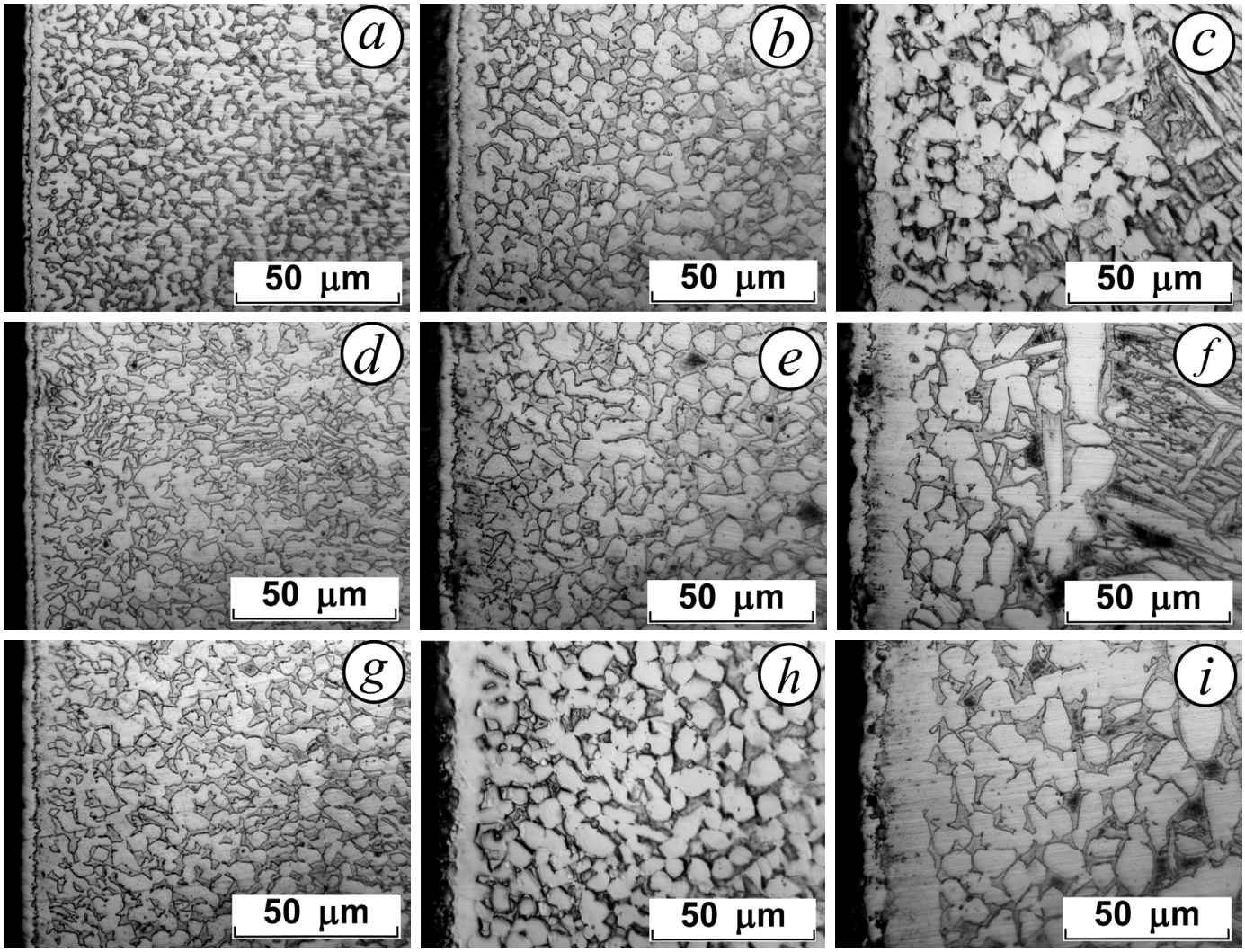

Fig. 7. The structures of near-surface layers of FT01 alloy depend on the temperature: 750°C – *a, d, g*; 800°C – *b, e, h*; 850°C – *c, f, i* and time parameters of nitriding: 2 h – *a, b, c*; 4 h – *d, e, f*; 8 h – *g, h, i*

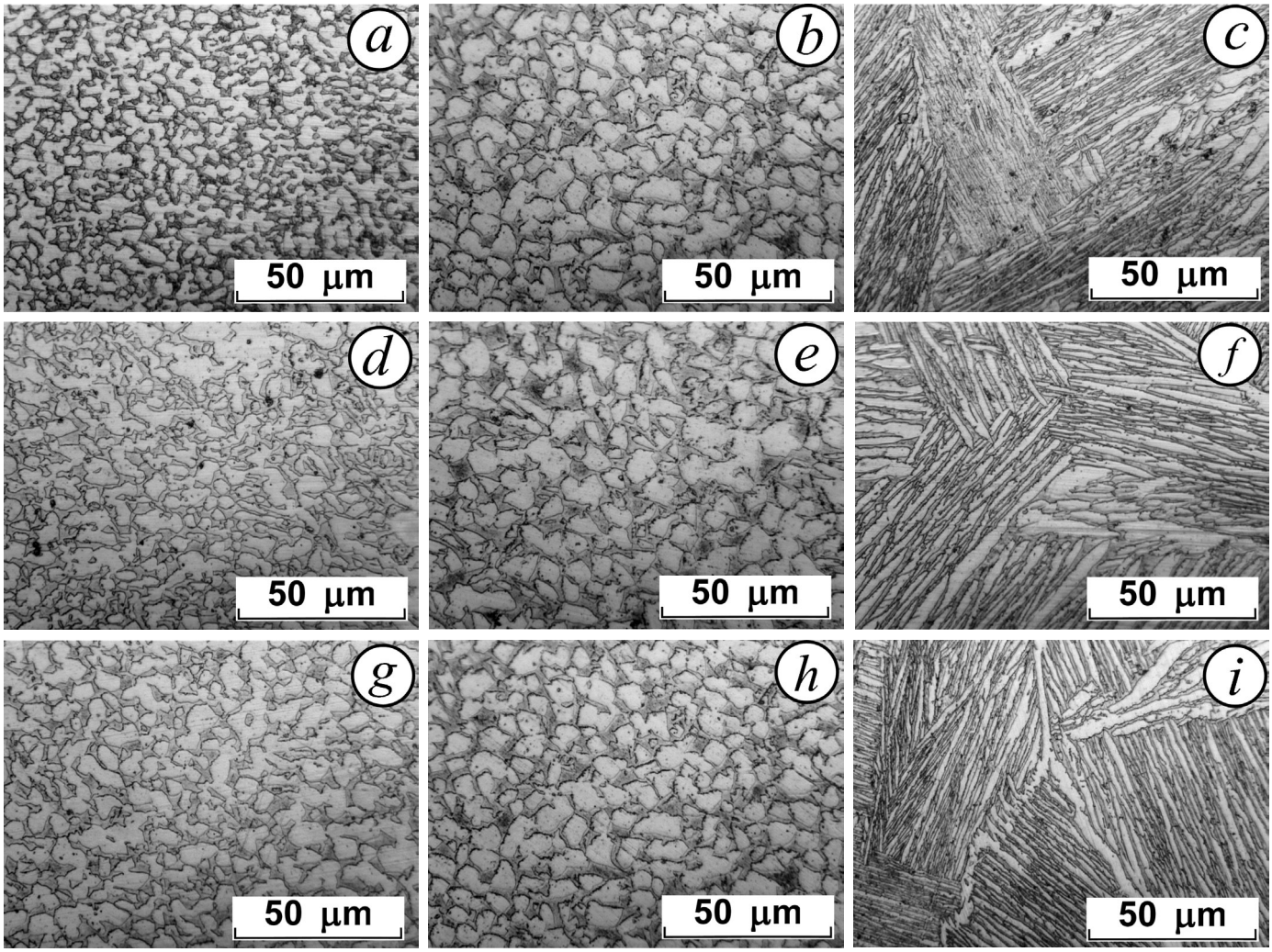

Fig. 8. The structure of FT01 alloy matrix depends on temperature: 750°C – *a, d, g*; 800°C – *b, e, h*; 850°C – *c, f, i* and time parameters of nitriding: 2 h – *a, b, c*; 4 h – *d, e, f*; 8 h – *g, h, i*

fusion distance, D is the nitrogen diffusion coefficient in the alloy, and τ is the diffusion time. The authors determined the effective nitrogen diffusion coefficient in the FT01 titanium alloy using the Arrhenius law (Fig. 10) and the kinetic dependences: $D_{ef} = D_0 \times \exp(-E/RT)$, where $D_0 = 0.0177$ m^2/s; $E = 215.7$ kJ/mol. The effective diffusion coefficient parameters are comparable with those published by Zhecheva et al. [21] and nitrogen diffusion in β-titanium [22]. The depth of hardened layers after nitriding in the studied temperature-time range of

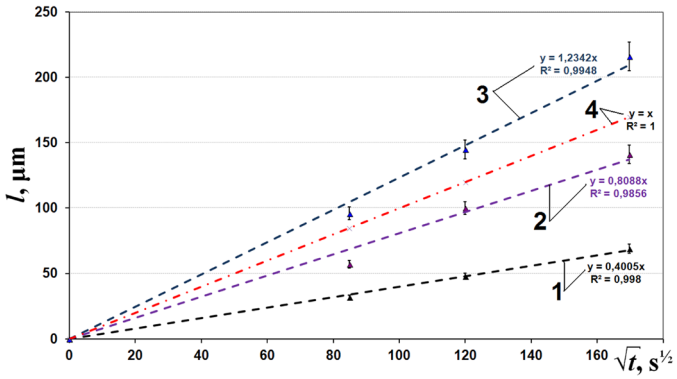

Fig. 9. The kinetics of hardened near-surface layer growth on FT01 titanium alloy by nitrogen gas interaction at temperatures: 1 – 750°C; 2 – 800°C; 3 – 850°C; 4 – the classic parabolic law curve

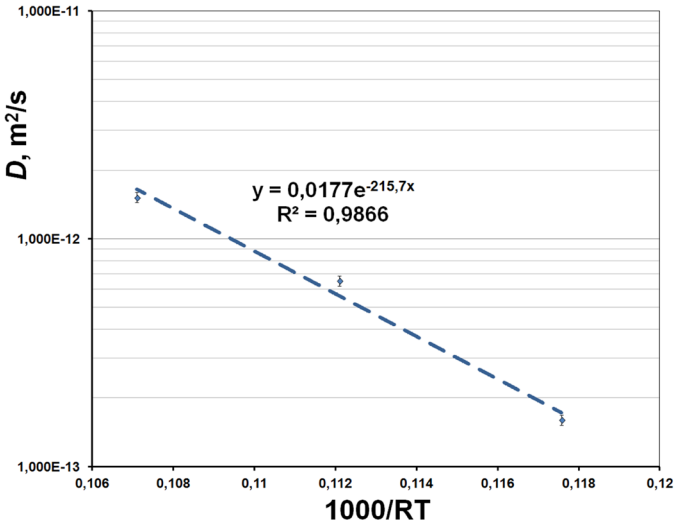

Fig. 10. The temperature dependence of the effective nitrogen diffusion coefficient in FT01 titanium alloy at 10^5 Pa of nitrogen gas pressure

parameters is 30...220 μm, according to the results of the durometric analysis. In addition to the surface hardness and depth of the hardened zone, the distribution of microhardness at the section of near-surface hardened layers demonstrates the level of surface hardening after diffusion saturation with nitrogen. As the temperature-time saturation parameters increase, the microhardness distribution curves migrate to the range with higher hardness values: the increase in hardness is higher with growing saturation temperature than with increasing exposure time (Fig. 11).

The gas nitriding (800°C, 8 h) of FT01 alloy discs for tribological tests in combination with a bronze block strengthens near-surface layers and changes the roughness and microhardness parameters of disc friction surfaces (see TABLE 4). The friction coefficient is lowered by significantly more than 10 times and the temperature in the friction zone is reduced by 2.5 times as a result of gas nitriding FT01 near-beta-titanium alloy (Fig. 12).

TABLE 4

The roughness (*Ra*) and microhardness ($HV_{0.49}$) parameters of friction surfaces of FT01 alloy discs before and after 8 h of gas nitriding at 800°C

***Ra*, μm**		**$HV_{0,49}$, GPa**	
Before Nitriding	After Nitriding	Before Nitriding	After Nitriding
0,19±0,05	0,25±0,03	3,5±0,1	11,3±0,05

4. Summary and conclusions

The researchers establish the surface hardening regularities of the near-beta-titanium alloy of the Ti-Al-V-Mo-Zr-Fe-Nb alloying systems after nitriding in gaseous nitrogen at 10^5 Pa pressure in the temperature range 750...850°C for a duration of 8 h. After nitriding in the studied temperature-time parameters, a 1...5 μm thick nitride layer is formed on the alloy's surface, consisting of nitrides of the parent metals TiN_x and Ti_2N. The activation energy for the formation of a nitride layer is ~108 kJ/mol. The surface roughness of the alloy degrades more strongly (by two roughness classes) at nitriding temperatures increased from 750 to 850°C than when saturation time is increased from 2 to 8 h (by one roughness class). The microhardness of the alloy surface is within 7...16 GPa after nitriding at the studied temperature-time parameters. In the studied temperature-time parameter range, the depth of hardened (diffusion) layers after nitriding of the near-beta-titanium alloy of the Ti-Al-Nb-Fe-Zr-Mo-V system is 30...220 μm. This layer's growth is controlled by the parabolic law. For the near-beta-titanium alloy of the Ti-Al-Nb-Fe-Zr-Mo-V alloying systems in the studied temperature-time range, the temperature dependence of the effective nitrogen diffusion coefficient in the alloy was calculated as $D_{ef} = D_0 \times \exp(-E/RT)$, where D_0 = 0.0177 m^2/s; E = 215.7 kJ/mol. The friction coefficient of the disk from FT01 near-beta-titanium alloy with

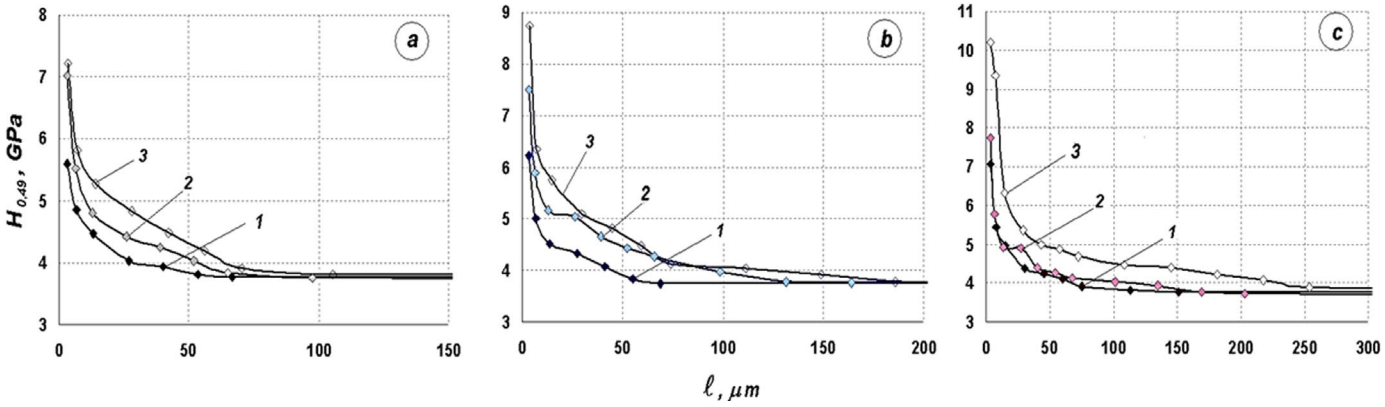

Fig. 11. The distribution of microhardness in the near-surface layers of FT01 titanium alloy after nitriding for 2 h (*a*), 4 h (*b*), and 8 h (*c*) at temperatures: *1* – 750°C, *2* – 800°C, and *3* – 850°C

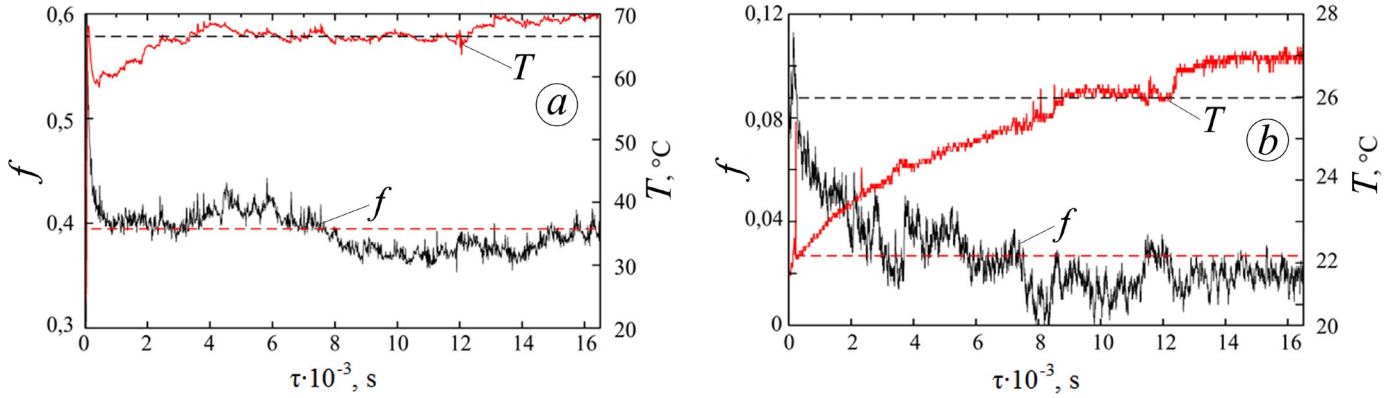

Fig. 12. The friction coefficient and temperature in the friction zone of an FT01 disk with a bronze block are before (*a*) and after (*b*) nitriding at 800°C with duration 8 h

a bronze block is lowered by significantly more than 10 times after gas nitriding, and the temperature in the friction zone is reduced by 2.5 times.

REFERENCES

[1] J.D. Cotton, R.D. Briggs, R.R. Boyer, S. Tamirisakandala, P. Russo, N. Shchetnikov, J. Fanning, State of the Art in Beta Titanium Alloys for Airframe Applications, JOM **67** (6), 1281-1303 (2015). DOI: https://doi.org/10.1007/s11837-015-1442-4

[2] H. Chang, L. Zhou, Current Situation of Titanium Research, Development and Applications in China, in: Proceedings of the 14th World Conference on Titanium (Ti 2019), MATEC Web of Conferences **321**, 01001 (2020). DOI: https://doi.org/10.1051/matecconf/202032101001

[3] A. Alexandrov, New research and development of titanium production and application in the CIS, in: Proceedings of the 14th World Conference on Titanium (Ti 2019), MATEC Web of Conferences **321**, 01002 (2020). DOI: https://doi.org/10.1051/matecconf/202032101002

[4] R.P. Kolli, A.A. Devaraj, A Review of Metastable Beta Titanium Alloys, Metals **8**, 506 (2018). DOI: https://doi.org/10.3390/met8070506

[5] H. Dong, Tribological properties of titanium-based alloys, in: Surface Engineering of Light Alloys. Aluminium, Magnesium and Titanium Alloys. Woodhead Publishing Series in Metals and Surface Engineering. Woodhead Publishing, pp. 58-80 (2010). ISBN 978-1-84569-537-8.

[6] O. Tisov, M. Łępicka, Y. Tsybrii, A. Yurchuk, M. Kindrachuk, O. Dukhota, Duplex Aging and Gas Nitriding Process as a Method of Surface Modification of Titanium Alloys for Aircraft Applications, Metals **12**, 100 (2022). DOI: https://doi.org/10.3390/met12010100

[7] T. Fraczek, R. Prusak, M. Ogórek, Z. Skuza, The Effectiveness of Active Screen Method in Ion Nitriding Grade 5 Titanium Alloy. Materials. **14**, 3951 (2021). DOI: https://doi.org/10.3390/ma14143951

[8] A. Edrisy, Kh. Farokhzadeh, Plasma Nitriding of Titanium Alloys, In Plasma Science and Technology: Progress in Physical States and Chemical Reactions, edited by Tetsu Mieno, London: IntechOpen 2016. DOI: https://doi.org/10.5772/61937

[9] A.M. Kamat, S.M. Copley, A.E. Segall, J.A. Todd, Laser-Sustained Plasma (LSP) Nitriding of Titanium: A Review, Coatings **9**, 283 (2019). DOI: https://doi.org/10.3390/coatings9050283

[10] S. Takesue, S. Kikuchi, H. Akebono, T. Morita, J. Komotori, Characterization of surface layer formed by gas blow induction heating nitriding at different temperatures and its effect on the fatigue properties of titanium alloy, Results in Materials **5**, 100071 (2020). DOI: https://doi.org/10.1016/j.rinma.2020.100071

[11] J. Kim, W.J. Lee, H.W. Park, Mechanical properties and corrosion behavior of the nitriding surface layer of Ti-6Al-7Nb using large pulsed electron beam (LPEB), Journal of Alloys and Compounds (2016). DOI: https://doi.org/10.1016/j.jallcom.2016.04.060

[12] L.A. Dobrzański, K. Gołombek, K. Lukaszkowicz, Physical Vapor Deposition in Manufacturing, in: Handbook of Manufacturing Engineering and Technology, A.Y.C. Nee (ed.), Springer-Verlag London 2015. P. 2719-2754. DOI: https://doi.org/10.1007/978-1-4471-4670-4_29

[13] L.A. Dobrzanski, D. Pakula, M. Staszuk, Chemical Vapor Deposition in Manufacturing, in: Handbook of Manufacturing Engineering and Technology, A.Y.C. Nee (ed.), Springer-Verlag London 2015. P. 2755-2803. DOI: https://doi.org/10.1007/978-1-4471-4670-4_29

[14] A. Zhecheva, W. Sha, S. Malinov, A. Long, Enhancing the microstructure and properties of titanium alloys through nitriding and other surface engineering methods. Surf. Coat. Tech. **200**, 2192-2207 (2005). DOI: https://doi.org/10.1016/j.surfcoat.2004.07.115

[15] S.X. Liang, L.X. Yin, X.Y. Liu, X.X. Wu, M.Z. Ma, R.P. Liu, Kinetics of thermodiffusion of TZ20 titanium alloy gas-nitride within temperature of 500°C-650°C. J. Alloy Compd. **734**, 172-178 (2018). DOI: https://doi.org/10.1016/j.jallcom.2017.11.052

[16] Ch. Yang, J. Liu, Intermittent vacuum gas nitriding of TB8 titanium alloy, Vacuum. **163**, 52-58 (2019). DOI: https://doi.org/10.1016/j.vacuum.2018.11.059

[17] V.M. Fedirko, I.M. Pohrelyuk, O.H. Luk'yanenko, S.M. Lavrys', M.V. Kindrachuk, O.I. Dukhota, O.V. Tisov, V.V. Zahrebel'nyi, Thermodiffusion Saturation of the Surface of VT22 Titanium Alloy from a Controlled Oxygen–Nitrogen-Containing Atmosphere in the Stage of Aging, Materials Science **53**, 691-701 (2018). DOI: https://doi.org/10.1007/s11003-018-0125-z

[18] I.M. Pohrelyuk, M.V. Kindrachuk, S.M. Lavrys', Wear Resistance of VT22 Titanium Alloy After Nitriding Combined with Heat Treatment. Materials Science **52**, 56-61 (2016). DOI: https://doi.org/10.1007/s11003-016-9926-0

[19] I. Weiss, S.L. Semiatin, Thermomechanical processing of beta titanium alloys – an overview, Materials Science and Engineering **A243**, 46-65 (1998). DOI: https://doi.org/10.1016/S0921-5093(97)00783-1

[20] E. Fromm, G. Hörz, Hydrogen, nitrogen, oxygen, and carbon in metals, Int. Metals Rev. **25**, 269-311 (1980). DOI: https://doi.org/10.1179/imtr.1980.25.1.269

[21] A. Zhecheva, S. Malinov, I. Katzarov, W. Sha, Modelling of kinetics of nitriding titanium alloys, Surf. Eng. **22**, 452-454 (2006). DOI: https://doi.org/10.1179/174327806X124717

[22] J. Xu, C.D. Lane, J. Ou, S.L. Cockcroft, D.M. Maijer, A. Akhtar, Y. Marciano, Diffusion of nitrogen in solid titanium at elevated temperature and the influence on the microstructure, Journal of Materials Research and Technology **12**, 125-137 (2021). DOI: https://doi.org/10.1016/j.jmrt.2021.02.073